CFD Analysis of Mine Fire Smoke Spread and Reverse Flow Conditions

J. C. Edwards and C. C. Hwang
Pittsburgh Research Laboratory
National Institute for Occupational Safety and Health
Pittsburgh, PA 15236
U.S.A.

ABSTRACT

A Computational Fluid Dynamics (CFD) program was used to model buoyancy induced Product-Of-Combustion (POC) spread from experimental fires in the National Institute For Occupational Safety And Health (NIOSH), Pittsburgh Research Laboratory (PRL), safety research coal mine. In one application, the CFD program was used to predict spread from fires in an entry under zero airflow conditions. At a location, 0.41 m below the entry's roof at a distance of 30 m from the fire, the measured smoke spread rates were 0.093 and 0.23 m/s for a 30 and a 296 kw fire, respectively. The CFD program predicted spread rates of 0.15 and 0.26 m/s based upon the measured fire heat production rates. Based upon a computation with c_3h_8 as the hydrocarbon fuel, a predicted 5 PPM co alert time of 70 s at a distance of 30 m from the fire is to be compared with the measured alert time of 148 s. In a second application, the CFD program was used to analyze smoke flow reversal conditions, and the results were compared with visual observations of smoke reversal for 12 diesel fuel fires. The CFD predictions were in qualitative agreement with visual observations of smoke reversal.

KEYWORDS

Computational Fluid Dynamics, Mine Fire, Smoke Spread, and Flow Reversal.

INTRODUCTION

Previous research (Edwards, *et al.,* 1997) has examined Product-of-combustion POC spread from 30 and 330 kW diesel fuel fires in a mine entry. The rate of POC spread is significant for establishing sensor spacing requirements in a mine for low airflow conditions. It was shown for 30 and 330 kW fires in a single entry how sensor spacings could be determined for zero airflow conditions based upon a CO alert of 5 ppm. For airflow velocities between 1 and 8 m/s and entry cross sectional area between 7 and 46 m^2 recommendations (Litton, *et al.,* 1991) were made for CO alarm levels for selected sensor spacings of 305 and 610 m.

Toxicity and visibility restrictions of smoke are two of its imminent hazard characteristics for miners in the event of a mine fire. The ability to predict smoke's movement under positive ventilation conditions is necessary for miner evacuation planning and mine fire control. Previous research (Lee, *et al.,* 1979; Kennedy, *et al.,* 1996) has examined one-dimensional Froude modelling to predict critical airflow conditions for the development of a buoyant roof layer countercurrent to the airflow. Their study was conducted in a laboratory scale tunnel with a 0.084 m^2 entry cross section. Additional research (Hwang and Wargo, 1986) investigated the formation and extent of the reversed stratified layer in a tunnel fire.

The availability of computational programs which efficiently solve the time dependent three-dimensional transport equations with turbulent chemically reactive buoyant flow provide an opportunity to analyze the transport of POC under zero airflow conditions and the onset of flow reversal. Two major advantages the computational fluid dynamics (CFD) programs provide are the flexibility to include various levels of approximation to the physical problem under investigation and the opportunity to study the effect of physical scale on the problem. The program selected, Adaptive Research's CFD2000,[1] includes a library of multiple step chemical reactions and a choice between laminar flow and turbulent flow described by the κ-ε model.

[1] Reference to a specific product does not imply endorsement by NIOSH.

Convective, conductive, and radiative heat exchange are part of the program. For the applications considered here, radiative heat exchange was not considered. The program is and selection of finite difference method and numerical convergence criteria.

MODEL DESCRIPTION

The governing transport equations are expressed as partial differential equations.
mass conservation:

$$\frac{\partial \rho}{\partial t} + \frac{\partial(\rho U_i)}{\partial x_i} = S_{m,p} \qquad (1)$$

momentum equation:

$$\frac{\partial(\rho U_i)}{\partial t} + \frac{\partial(\rho U_i U_j)}{\partial x_j} = -\frac{\partial p}{\partial x_i} - \frac{\partial \tau_{ij}}{\partial x_j} + S_{Ui} + S_{Ui,p} \qquad (2)$$

energy conservation:

$$\frac{\partial \rho h}{\partial t} + \frac{\partial(\rho U_j h)}{\partial x_j} = \frac{\partial p}{\partial t} + U_j \frac{\partial p}{\partial x_j} + \frac{\partial}{\partial x_j}\left[\left(\frac{\mu}{\mathrm{Pr}} + \frac{\mu_t}{\mathrm{Pr}_t}\right)\frac{\partial h}{\partial x_j}\right] + S_h + S_{h,p} \qquad (3)$$

scalar conservation:

$$\frac{\partial \rho \phi}{\partial t} + \frac{\partial(\rho U_j \phi)}{\partial x_j} = \frac{\partial}{\partial x_j}\left[\Gamma \frac{\partial \phi}{\partial x_j}\right] + S\phi \qquad (4)$$

gas equation of state:

$$P = \rho \frac{Rg}{W} T \qquad (5)$$

where x_i = position vector in the i^{th} coordinate direction

t = time
ρ = local fluid density
T = local fluid temperature
U_i = i^{th}- fluid velocity component
P = fluid pressure
h = density weighted enthalpy
$S_{m,p}$ = rate per unit volume at which mass is transferred to the fluid
S_{Ui} = i^{th} component of body force per unit volume (e.g., gravity)
$S_{Ui,p}$ = momentum source/sink term
μ = laminar dynamic viscosity
μ_t = turbulent dynamic viscosity
$\tau_{i,j}$ = viscous stress tensor
ϕ = scalar quantity
Γ = diffusion coefficient for quantity ϕ
S_h = heat production per unit volume
$S_{h,p}$ = enthalpy source/sink term
$S\phi$ = source/sink term for quantity ϕ
R_g = gas constant

The general scalar quantity ϕ represents diverse physical variables such as mass fraction of gas species; turbulent kinetic energy; and turbulent kinetic energy dissipation rate. The source term $S\phi$ in the case of chemical reactions is an exponential function of reciprocal temperature in the form of an Arrhenius reaction.

Utilization of the computer program requires specification of the system's geometry, dimensions, spatial grid resolution, fluid physical properties and equation of state, inlet and outlet boundary conditions, wall boundary conditions, chemical reaction rate scheme, laminar or turbulent flow, and time step. Various finite difference representations of the governing partial differential equations are available for use in the computational program depending upon the flow regime. The solution algorithm is pressure implicit with splitting of operators. The controlling parameter in application of the equations is the time step. For chemically reactive flows the reaction rate will determine the time step. For unsteady nonreactive flows, the Courant-Friedrichs-Lewy (CFL) condition restricts the time step.

RESULTS

The mine section considered is shown in Figure 1. Table 1 lists the experimental conditions for experiment Nos. 1-2 with a fire at position F1 in F-Butt and Nos. 3-14 with a fire at position F2 in room 10. Experiment Nos. 1 and 2 were conducted under zero airflow conditions, and experiment Nos. 3-14 were conducted under positive airflow conditions with a linear airflow v_i in the fire zone. The brattice at room 10 and B-Butt was used to regulate the airflow through the fire at F2. The mass loss rate $\dot{m}$ of the diesel fuel was assumed to be uniform over the duration of the observed burn time. The linear fuel burn rate is v_l . Physical properties of

the diesel fuel are its mass density of 876. kg/m^3, heat of combustion 42x10^3 kJ/kg, and the combustion efficiency of 0.84. The measured diesel fuel burn time was used to estimate the gas injection velocity v_g into the entry from the pan with the assumption that the hot vapor

Table 1. Experimental Conditions.

Exp.	Fuel, L	Pan, m^2	$\dot{m}$, kg/s	v_l, m/s	v_g, m/s	$\dot{Q}$, kW	v_i, m/s
1	24	0.37	0.0089	2.6e-5	0.086	296	0
2	3	0.047	0.000866	2.1e-5	0.069	30	0
3	3	0.21	0.0022	1.2e-5	0.039	77	0.49
4	2	0.047	0.00051	1.2e-5	0.041	18	0.43
5	1	0.047	0.00056	1.4e-5	0.045	20	0.41
6	1	0.047	0.00081	2.0e-5	0.065	29	0.24
7	1	0.047	0.00059	1.4e-5	0.047	21	0.37
8	1	0.047	0.00078	1.9e-5	0.062	28	0.2
9	1.5	0.21	0.0015	3.6e-5	0.12	93	0.32
10	0.7	0.047	0.00054	1.3e-5	0.043	19	0.32
11	1	0.21	0.0011	2.7e-5	0.088	38	0.3
12	0.5	0.047	0.00049	1.2e-5	0.039	16	0.3
13	1	0.21	0.0022	5.3e-5	0.18	77	1.17
14	0.55	0.047	0.00035	8.5e-6	0.028	12	1.17

temperature was 1,000 °C. A square pan was used to contain the fuel in experiment Nos. 1, 3, and 9-11. In the remaining experiments, a cylindrical bucket was used.

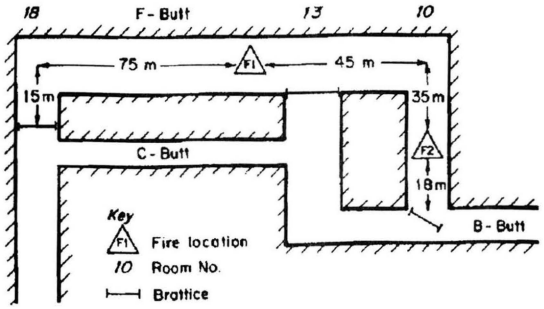

Figure 1. Plan view of mine section.

A small quantity of gasoline, about 250 mL, was added to the diesel fuel to initiate a uniform burning of the liquid. For the zero airflow experiments Nos. 1 and 2, the spread of the CO laden fire product gases was evaluated with a CO monitor suspended from the mine entry roof with the sensor's diffusion tube inlet about 0.41m below the roof. For experiment Nos. 3-14, visual observations were made of the extent of the roof layer reverse flow.

For experiment Nos. 1 and 2, the measured first arrival of CO at stations 30 m upwind and downwind of the fire at F1 were used to determine an average flow velocity. The measured average velocities were 0.093 and 0.23 m/s for the fire intensities of 30 and 296 kW, respectively. The experimental conditions were simulated with CFD2000 for an entry with average height and width of 2 m and 4.6 m extending 30 m in either direction from F1. The output boundary conditions at either end of the entry were specified as zero gradient boundary conditions for the pressure, and ambient temperature. The boundary condition along the entry roof, ribs, and floor were specified as no slip flow and zero heat flux conditions. At the diesel fuel fire source the gas velocity v_g and heat production rate $\dot{Q}$ were specified by the values in table 1. The time step is automatically computed from the CFL conditions as the computation progressed. For experiment Nos. 1 and 2, the predicted airflow velocities are 0.26 and 0.15 m/s, respectively. For the 296 kW fire of experiment No. 1 the predicted value exceeds the measured value by 13 pct, and for the 30 kW fire of experiment No. 2 the predicted value exceeds the measured value by 61 pct. It is expected that the predicted velocity would be higher since the incompressible movement of the air by the heat source of the fire which acts as a piston will effect a disturbance before the measurable POC have been transported to the sensor station.

The plume of hot buoyant gas, which rises from the fire source, generates a moving roof layer of POC which increases in thickness due to turbulent mixing with the cooler air in the entry. Figures 2 and 3 show the computed fire plume growth as represented by the gas temperature T and vertical velocity V component 0.41 m below the roof at Y=1.59 m, where Y is the vertical distance above the floor, and 0.41 m above the floor at Y=0.41 m at the geometric center of the fire zone for experiment Nos. 1 and 2. Ignition of the fuel occurred at time zero. These results also show that the fire plume growth reaches a steady state within 5 and 4 min, respectively. For the less intense 30 kW fire of experiment No. 2 there is a greater oscillatory behavior exhibited by the fire temperature and vertical component of the gas velocity than for the more intense 296 kW fire during the initial 5 minute transient. This is probably a consequence of the reduced buoyant force of the hot gas compared to the frictional drag of the surrounding air.

The temperature 30 m upwind and downwind of the fire was measured for experiment No.1 at a distance 0.41 m below the roof with a thermocouple. Figure 4 shows

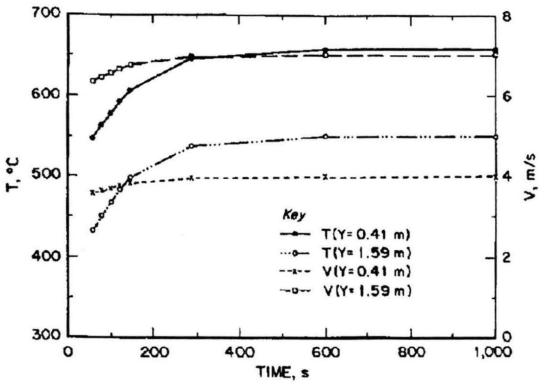

Figure 2. Predicted gas temperature and vertical gas velocity 0.41 m above geometric center of fire zone and 0.41 m below roof for experiment No. 1.

a comparison of the model computed temperature and the average measured temperature at the two stations. The predicted temperature is greater than the measured temperature in the first 1,000 s. This is expected since the computed transport velocity is higher than the measured velocity, and heat loss at the roof into the coal is neglected with the assumption of an adiabatic boundary at the roof.

This application of the CFD2000 program utilized the experimentally observed measured heat flux as a source of the buoyant roof layer. A disadvantage of this method is the lack of information about the spread of the POC generated by the fire. Air movement will be produced at a distance from the fire prior to the POC arrival. Another approach to the problem is to model the chemical kinetics of a fire. For this application, a four step reaction rate chemistry model of C_3H_8, which was selected from the CFD2000 program library to represent the fuel, with air was evaluated for the fire pan size and injection velocity of fuel in experiment No. 1. Propane (C_3H_8) has a heat of combustion of 46. X 10 ^{3} kJ/kg, which is similar to diesel fuel. The heat generation rate is no longer a prescribed quantity, but is a result of the reaction kinetics and oxygen

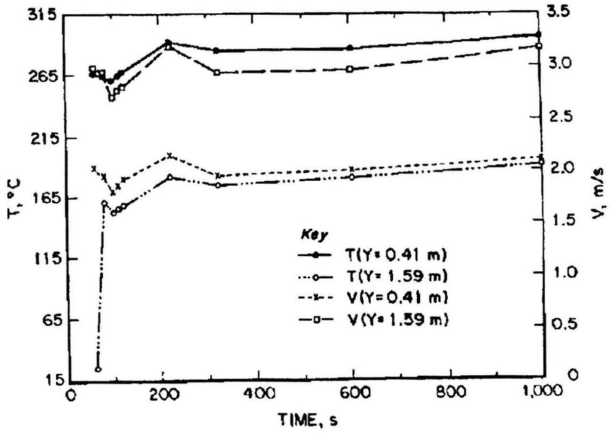

Figure 3. Predicted gas temperature and vertical gas velocity 0.41 m above geometric center of fire zone and 0.41 m below roof for experiment No. 2.

consumption. The predicted CO, at a distance of 30 m from the fire and 0.41 m below the roof, is compared with the CO measured by a diffusion mode CO sensor 30 m in either direction from the fire in figure 5. Sensor CO8 is on the room 10 side of F1, and sensor CO13 is on the room 18 side of F1. The CO sensor is limited to read a maximum CO concentration of 50 ppm. The average arrival time of the measured CO concentration of 5 ppm above ambient is

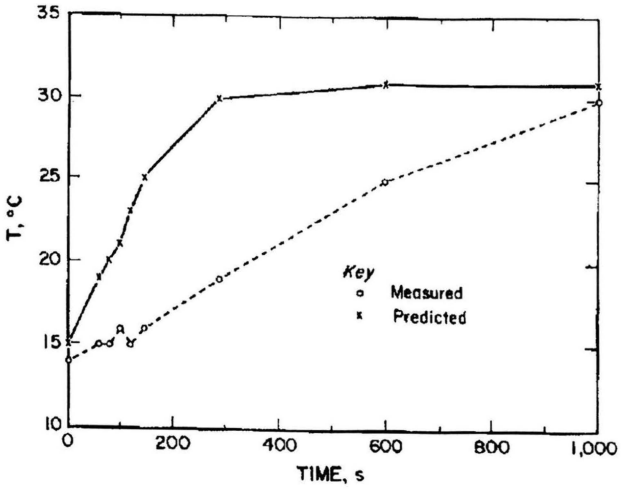

Figure 4. Predicted and measured gas temperature 30 m from the fire for experiment No. 1.

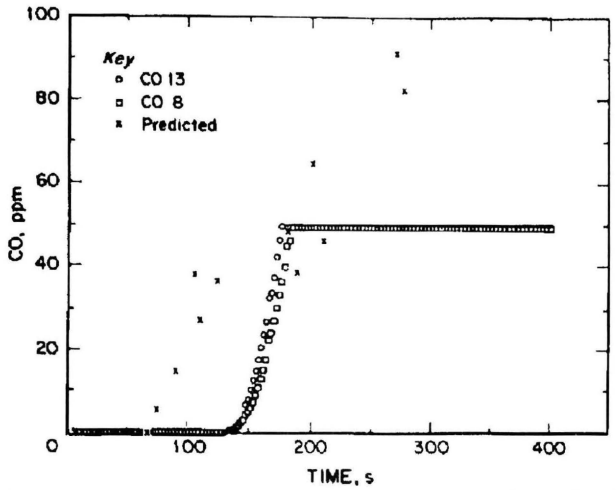

Figure 5. Predicted and measured CO 30 m from the fire for experiment No. 1.

148 s, whereas the predicted CO concentration of 5 ppm is 70 s. Part of the discrepancy between measured and predicted CO concentration is a result of the 35 s response time of the sensor cell, and part is due to the average fuel injection rate used for the calculation which does not account for the transient fire growth. The fuel injection rate will depend upon the radiative and convective heat flux from the flame zone to the fuel surface. This coupled nonlinear process is not accounted for in this application of the model with a defined fuel injection velocity.

Experiment Nos. 3-14 represent diesel fuel fire experiments conducted with the fire source located at position F2. Table 2 shows the fire size varied between 12 and 93 kW. The average linear airflow at the fire zone measured prior to the fire varied between 0.2 and 1.17 m/s. A visual observation was made of the extent of the smoke reversal from each experiment. For experiment Nos. 3-5, 7, 9-10, and 12 a roof layer backup of 7 to 12 m was observed. The observed roof layer backup for experiment Nos. 6, 8, and 11 was greater than 18.4 m and extended into B-Butt. There was no smoke backup in experiment Nos. 13 and 14. These results were compared with two models. The first model is a one-dimensional Froude model (Kennedy, *et al.,* 1996), and the second is the detailed three-dimensional calculation with the CFD2000 program. The Froude number Fr is defined in terms of the ratio of the buoyancy force to the inertia force in a fluid. For a constant pressure regime:

$$\mathrm{Fr} = \frac{gH}{V^2}\left(1 - \frac{T}{T_f}\right) \qquad (6)$$

where T_f = average temperature of fire site gas
T = ambient air temperature
H = entry height
g = acceleration due to gravity
V=air velocity.

The quantity T_f is defined in terms of the air mass flow rate $\dot{m}$ upwind of the fire through the relationship:

$$T_f = T + \frac{\dot{Q}}{\rho A V c_p} \qquad (7)$$

where $\dot{Q}$ = fire heat production rate
c_p = air specific heat
A = entry cross sectional area at fire location.

If Fr is less than some critical value reverse flow will not occur. It was shown (Lee, *et al.*, 1979a, 1979b) that the critical Froude number range was between 4.5 and 6.7. This is equivalent to stating that if the air velocity is greater than some critical velocity V_c then reverse flow does not occur. Figure 6 shows V_c calculated from equations 6 and 7 for Fr = 4.5 and 6.7 over a range of fire intensities from 10 to 500 kW. The roof layer backup greater than 18.4 m observed for experiment Nos. 6, 8, and 11 occurred for a ventilation air flow less than V_c for Fr=6.7.

Application of the CFD2000 program was made to determine the onset of reverse flow within 0.20 m of the mine roof near a fire source for six fire heat release rates $\dot{Q}$ at position F2. At F2 the entry height and width are 2 m and 3.88 m. The conditions for the fire sources are shown in table 2. Geometrically, the fire source was represented as a square surface area on the floor. The inlet air velocity was specified 30 m upwind of the fire source. This calculation was intended to detect incipient flow reversal at the fire zone. For this purpose V_c was defined as the linear inlet velocity below which airflow reversal was initiated at

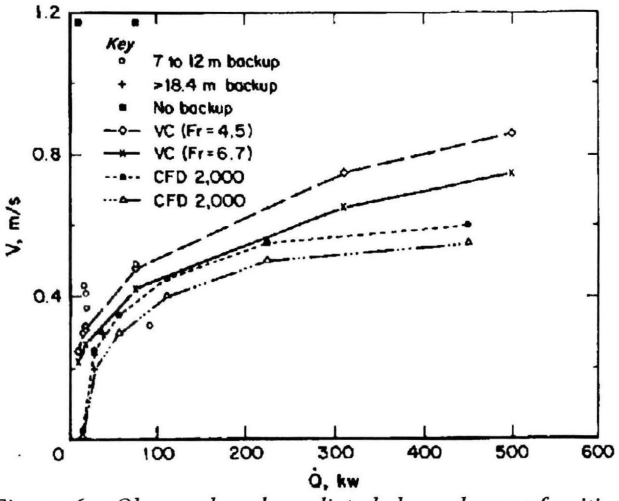

Figure 6. Observed and predicted dependence of critical velocity for smoke reversal on heat flux for experiment Nos. 3-12.

fire zone edge. Through trial computations, the value of V_c was bracketed. The results of the calculations are presented in figure 6. The CFD critical velocity values are lower than those determined by the one-dimensional Froude model for Fr = 6.7. The extensive smoke backup of experiment Nos. 6, 8, and 11 are predicted more favorably by the Froude model than the CFD2000 model. The Froude model and CFD results appear to diverge at higher fire intensities. The criterion that the predicted flow reversal is defined by a reversal at the leading edge of the fire pan is modified by a consideration of the fire induced recirculatory flow upwind of the pan. For example, the CFD2000 computations showed that a 28 kW fire generates a recirculation zone near the roof which extends 6 m upwind of the fire for an inflow air velocity of 0.25 m/s,

Table 2. CFD2000 critical velocity.

Case	Fire area, m^2	$\dot{Q}$, kW	V_c, m/s
A	0.0234	14	0.01-0.025
B	0.0471	28	0.20-0.25
C	0.0942	56	0.30-0.35
D	0.188	112	0.40-0.45
E	0.377	225	0.50-0.55
F	0.753	449	0.55-0.60

although there is no reversal of airflow at the exact edge of the fuel pan. Smoke transfer from the bent fire plume into the recirculatory zone would increase the model predicted critical velocity.

CONCLUSIONS

The computational program CFD2000 was used to simulate buoyant roof layer flow generated by a diesel fuel fire in a mine entry under zero airflow conditions in two experiments. For a 296 kW and a 30 kW fire, the computational program predicted fire induced air velocities near the roof, which overestimated the POC measured spread rates. The overestimation is a result of not distinguishing the POC from the airflow in the computation. The predicted gas temperature near the roof 30 m from a 296 kW fire was higher than the measured values. This is a result of not including heat loss to the mine roof. When the CFD2000 program was used to model the CO generated by a hydrocarbon (C_3H_8) fire source, the qualitative agreement of the predicted and measured CO concentration was good, although the predicted time for a CO alert value of 5 ppm 30 m upwind of the 296 kW fire occurred earlier than the measured alert time. This discrepency was in part due to the sensor response time, and in part due to the transient fire growth.

Application of the CFD2000 program to model the development of reverse flow conditions for a diesel fuel fire under positive ventilation conditions in a mine entry showed that the predicted critical velocity for reverse flow conditions was lower than predicted by a Froude model analysis. It was also determined that the measured extensive smoke reversal is more favorably predicted by the Froude model. The interpretation of smoke reversal as a reversal of the roof layer at the edge of the fire pan in the application of the CFD2000 program is possibly too stringent a definition of smoke reversal. Turbulent mass transfer of smoke from the ascending plume into a recirculatory zone established upwind of the fire would result in an increased critical velocity for reverse flow. Successful qualitative application of the CFD program is dependent upon a proper description of the experimental conditions. When there is incomplete information, the CFD program can still yield useful qualitative information with regard to the parametric influence of experimental conditions on CFD predictions.

REFERENCES

Edwards, J.C., Friel, G.F., Franks, R.A. and Opferman, J.J., 1997, "Mine Fire Detection Under Zero Airflow Conditions," *International Mine Ventilation Congress*, Pittsburgh, PA, May 17-22, pp. 331-336.

Hwang, C.C. and Wargo, J.D., 1986, "Experimental Study of Thermally Generated Reverse Stratified Layers in a Fire Tunnel," *Combustion and Flame* v. 66, pp. 171-180.

Kennedy, W.D., Gonzalez, J.A. and Sanchez, J.G., 1996, "Derivation and Application of the SES Critical Velocity Equations," *ASHRAE Transactions: Research* v. 102, no. 2, pp. 40-44.

Lee, C.K., Hwang, C.C., Chaiken, R.F. and Singer, J.M., 1979a, "Interaction Between Duct Fires and Ventilation Flow: An Experimental Study," *Combustion Science and Technology* v. 20, pp. 59-72.

Lee, C.K., Hwang, C.C., Singer, J.M. and Chaiken, R.F., (1979b), "Influence of Passageway Fires on Ventilation Flows," *International Mine Ventilation Congress*, Reno, NV, Nov. 4-8, pp. 448-454.

Litton, C.D., Lazzara, C.P. and Perzak, F.J., 1991, "Fire Detection for Conveyor Belt Entries," *U.S. Bureau of Mines Report of Investigations* 9380, 23 pp.